Algal Research 41 (2019) 101514

Contents lists available at ScienceDirect

Algal Research

journal homepage: www.elsevier.com/locate/algal

Effect of macronutrients on phospholipid production by the microalga *Nannochloropsis oculata* in a photobioreactor

Ahmet Y. Manisali[a], Aydin K. Sunol[a], George P. Philippidis[b,*]

[a] Chemical & Biomedical Engineering Department, University of South Florida, 4202 E. Fowler Ave., Tampa, FL 33620, USA
[b] Patel College of Global Sustainability, University of South Florida, 4202 E. Fowler Ave., Tampa, FL 33620, USA

ARTICLE INFO

Keywords:
Phospholipids
Nannochloropsis oculata
Macronutrients
^{31}P NMR spectroscopy

ABSTRACT

Concerns about greenhouse gas emissions and climate change have raised global demand for renewable products, leading to increased interest in sustainable resources. Microalgae constitute a potentially sustainable source of natural compounds, such as phospholipids, which are extensively used in cosmetics as part of liposomes, emulsifiers, solubilizers, and wetting agents. Currently phospholipids are extracted from food sources, a practice that raises sustainability concerns. Photosynthetic microalgae cultivated on nitrogen and phosphorus macronutrients may serve as a more sustainable source of the major phospholipids phosphatidylcholine, phosphatidylethanolamine, lyso-phosphatidylcholine, and lyso-ethanolamine. We assessed the effect of nitrogen and phosphorous provision on phospholipid production by the marine microalga *Nannochloropsis oculata* cultivated in a 3.5-liter flat panel photobioreactor at two macronutrient mass ratios, NO_3^-/PO_4^{3-} = 15 and NO_3^-/PO_4^{3-} = 5. Using organic solvent extraction and ^{31}P NMR spectroscopy, phospholipid content in cell mass was found to be 26% higher at the ratio of 5 than at the ratio of 15, indicating that phosphate-rich cultivation boosts phospholipid formation. Moreover, the specific growth rate of the culture at the ratio of 5 was higher than at the ratio of 15. After the growth phase the cultures were subjected to macronutrient starvation, a common practice for increasing total lipid production. Therefore, maintaining a NO_3^-/PO_4^{3-} ratio of 5 is deemed to be essential for exploiting microalgae for large scale production of phospholipids.

1. Introduction

Among microalgal products, lipids have been the most prominent ones because they can be readily converted to biodiesel, jet fuel, and other renewable fuels with large commercial potential [1–3]. However, lipid-derived biofuels are still not competitive with oil products because of the relatively low oil prices. As a result, research and commercial interest is directed towards algal specialty compounds of high value, which are also viewed as more sustainable compared to their counterparts derived from food products, given that algae do not compete with human food or animal feed. In particular, algal phospholipids can serve the needs of the cosmetics and nutraceutical industries for sustainable specialty products replacing phospholipids presently derived from food sources, mainly soybeans and eggs [4,5]. Phospholipids are polar lipids that are essential components of the cellular membrane of algae cells [6,7]. Certain phospholipids, such as phosphatidylcholine (PC), phosphatidylethanolamine (PE), lyso-phosphatidylcholine (lyso-PC), and phosphatidylinositol (PI), are used as key ingredients in emulsifiers, liposome formers, solubilizers, and wetting agents [6,8].

Total lipids, which comprise membrane polar lipids (phospholipids and glycolipids) and intracellular neutral lipids, usually constitute 15–35% of the algal cell mass on a dry basis and can be isolated from cell mass with the use of various methods employing solvents, such as chloroform, methanol, and hexane. The combination of chloroform and methanol are reported to be highly effective on algae [9–11]. The popular Folch method utilizes a 2:1 volumetric mix of chloroform and methanol for dissolving total lipids and water for removing non-lipid substances from the cell extract [12–14]. Polar lipids can subsequently be separated from neutral lipids and purified by combining the Folch extraction method with silica solid-phase extraction (SPE) [15,16].

Abbreviations: VFPPBR, vertical flat-panel photobioreactor; ATC, automatic temperature compensation; OD, optical density; NO_3-N, nitrate nitrogen; PO_4-P, phosphate phosphorus; R^2, correlation coefficient; X, dry cell mass concentration ($g{\cdot}L^{-1}$); N, cell concentration ($cells{\cdot}mL^{-1}$); μ_{max}, maximum specific cell growth rate (d^{-1}); P_v, average cell mass volumetric productivity ($g{\cdot}L^{-1}{\cdot}d^{-1}$); P_a, average cell mass areal productivity ($g{\cdot}m^{-2}{\cdot}d^{-1}$); Y_N, cell mass yield on nitrogen (g biomass per g NO_3-N); Y_P, cell mass yield on phosphorus (g biomass per g PO_4-P); SD, standard deviation

* Corresponding author.
E-mail address: gphilippidis@usf.edu (G.P. Philippidis).

https://doi.org/10.1016/j.algal.2019.101514
Received 3 January 2019; Received in revised form 22 March 2019; Accepted 22 April 2019
2211-9264/ © 2019 Elsevier B.V. All rights reserved.

Phospholipids can be analyzed by high performance liquid chromatography (HPLC) using various detectors, but accuracy is questionable [17,18]. On the other hand, nuclear magnetic resonance (NMR) spectroscopy, specifically ^{31}P NMR spectroscopy, can quickly and accurately quantify phosphorus compounds in cellular extracts without the need for labor-intensive sample processing or preparation [18,19].

The purpose of this study was to assess the phospholipid production potential of the promising marine microalga *N. oculata* by manipulating the relative provision of the macronutrients nitrogen (as NO_3^-) and phosphorus (as PO_4^{3-}) during cultivation in a photobioreactor. Using the Folch method for phospholipid extraction and ^{31}P NMR spectroscopy for quantification, the study was designed to test our hypothesis that a phosphorus-enriched medium will boost phospholipid production. Moreover, we examined whether macronutrient starvation after rigorous cell growth can further enhance phospholipid synthesis, a strategy reported in the literature [20–22] for boosting total lipid production aimed primarily for conversion to biofuels.

2. Materials and methods

2.1. Vertical flat panel photobioreactor

The vertical flat panel photobioreactor (VFPPBR) was constructed in-house with acrylic panels. The bioreactor had overall dimensions of 23.5 cm in width, 40.0 cm in length, and 5.0 cm in depth and was operated at a working volume of 3.5 L (Fig. 1). The design of the VFPPBR aims at maximizing light exposure, whereas its enclosed nature practically eliminates evaporative water loss and contamination risk. Vigorous mixing of the culture is accomplished with the use of aquarium bubble stones (Aqua Culture®, FL, USA) attached to the bottom of the reactor. The delivery of compressed CO_2 gas (Industrial Grade Carbon Dioxide, CGA-320, Airgas®), as carbon source, is controlled with an on-off switch valve activated when the culture's pH deviates from the set point of 7.50 ± 0.05. A pH sensor with automatic temperature compensation (ATC) is utilized to control the pH and record the temperature of the culture during operation.

2.2. Strain selection and cultivation conditions

The marine microalga *Nannochloropsis oculata* was selected for phospholipid production in the VFPPBR based on previous reports of high lipid productivity in the range 84–142 $mg{\cdot}L^{-1}{\cdot}d^{-1}$ [23] with a polar lipid fraction exceeding 15% of dry cell mass [24]. The strain was purchased from the UTEX Culture Collection of Algae (University of Texas, Austin) and was cultivated in artificial seawater medium containing Instant Ocean™ salt at 35 $g{\cdot}L^{-1}$ with commercially available Guillard's f/2 medium supplemented with nitrates and phosphates, as detailed in Table 1.

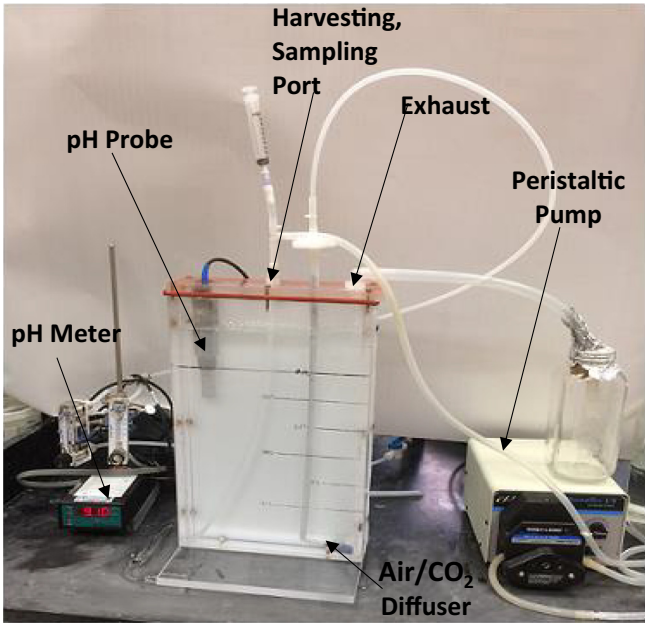

Fig. 1. Bench-scale vertical flat-panel photobioreactor (FPPBR).

Table 1
Initial composition of *N. oculata* growth medium. Nitrate (as $NaNO_3$) and phosphate (as $NaH_2PO_4{\cdot}H_2O$) salts were periodically supplemented to keep their concentrations above 200 $mg{\cdot}L^{-1}$ and 10 $mg{\cdot}L^{-1}$, respectively, during the growth phase.

Component	Concentration
Seawater[1]	$g{\cdot}L^{-1}$
Instant Ocean™	35
Macronutrients[2]	$mg{\cdot}L^{-1}$
$NaNO_3$	776
$NaHCO_3$	420
$NaH_2PO_4{\cdot}H_2O$	52
Vitamin[3]	$mg{\cdot}L^{-1}$
B12	0.0005
Biotin	0.0005
Thiamine HCl	0.10
Trace metals[3]	$mg{\cdot}L^{-1}$
$CoCl_2{\cdot}6H_2O$	0.01
$CuSO_4{\cdot}5H_2O$	0.01
$FeCl_3$	1.90
$MnCl_2{\cdot}4H_2O$	0.18
Na_2MoO_4	0.006
$ZnSO_4{\cdot}7H_2O$	0.022
$N_2Na_2O_8$	4.36

[1] Manufacturer recipe.
[2] Ben-Amotz [25].
[3] Manufacturer recipe (f/2 Guillard's marine enriched seawater without silicate).

The microalgae cultivation studies in the VFPPBR, conducted in duplicate, aimed at assessing the effect of macronutrient ratio on phospholipid production. More specifically, two ratios were tested, $NO_3^-/PO_4^{3-} = 15$ and $NO_3^-/PO_4^{3-} = 5$, by setting the initial concentration of nitrates (NO_3^-) at 566 $mg{\cdot}L^{-1}$ in both cases and varying the initial concentration of phosphates (PO_4^{3-}) appropriately to achieve the desired ratio. Each cultivation was conducted in two sequential phases: (1) A first phase during which NO_3^- and PO_4^{3-} were periodically supplemented at the respective ratio to ensure a macronutrient-rich environment by keeping their concentrations above 200 and 10 $mg{\cdot}L^{-1}$, respectively; and (2) After partially harvesting the culture, a second phase during which no subsequent supplementation of nitrates and phosphates was done to subject the cultures to macronutrient depletion and starvation.

At each macronutrient ratio, after the 3.5 L of culture reached the peak of its nutrient-rich growth phase, 2.0 L of culture were harvested to determine phospholipid production during this nutrient-rich phase through extraction and quantification, as detailed later. The remaining 1.5 L of culture, supplemented with 2.0 L of fresh medium to restore its volume to the original 3.5 L, were kept in the VFPPBR for further cultivation, but without any more macronutrient additions to evaluate the effect of macronutrient starvation on the phospholipid content of the cell mass. Using stock cultures, inoculum for the VFPPBR runs was prepared in 500-mL flasks cultivated at 23 °C in a rotary shaker operating at 150 rpm under continuous LED illumination. A 10% (v/v) inoculum from the flask culture was added to the bleach-sterilized VFPPBR with a working volume of 3.5 L. Air enriched with compressed CO_2 gas was bubbled through the VFPPBR as carbon source and for culture mixing. The pH was kept at 7.50 ± 0.05 by automatically altering the addition of compressed CO_2 to air through a controller.

Samples collected daily were used for monitoring cell growth, residual macronutrient concentration, and phospholipid production. The VFPPBR was exposed to artificial light via a LED light source at approximately 10–12 klx on a 16:8 h light:dark cycle and was maintained in an air-conditioned laboratory at 22 °C. The temperature within the VFPPBR was 30 ± 2 °C at all times.

2.3. Monitoring microalgal growth and macronutrient concentration

Cell growth was monitored by measuring in duplicate optical density, cell concentration, and dry cell weight. Optical density (OD_{680}) was measured at 680 nm, which is the wavelength suitable for chlorophyll-a absorption, utilizing a spectrophotometer (DU 730, Beckman Coulter, USA). Using an automated cell counter (Auto X4, Nexcelom, USA), we measured cell concentration (cells mL^{-1}). Dry cell weight (X), expressed in $g\,L^{-1}$, was measured by filtering a small volume (2.5–5.0 mL) of culture through pre-dried and pre-weighed 0.47 μm Whatman Grade nylon filters and then by placing the cell pellet in a moisture analyzer (MB25, Ohaus, USA) operated at 100 °C.

The residual concentrations of the macronutrient nitrates and phosphates in the culture were monitored daily in duplicate in the filtrate of the samples mentioned above using UV spectrophotometry at 220 nm and at 650 nm, respectively. Supplemental nitrates and phosphates were provided, when needed, during the growth phase of each cultivation to ensure that microalgal growth was not macronutrient-limited except during the intentional starvation phase.

2.4. Phospholipid extraction

The Folch method of lipid extraction from whole cells [14] was employed in the present study. The microalgae culture was first centrifuged at 7500 rpm and 10 °C for 10 min and then subjected to vacuum-oven drying at 60 °C. The dried cell mass was then pulverized by mortar and pestle and stored in sealed glass vials inside a desiccator. Total cellular lipids were extracted from 1.00 g of the powdered microalgal cell mass with the use of a mixture (12 mL) of the solvents chloroform and methanol at a volumetric ratio of 2:1. To ensure thorough mixing, the cell mass-solvent suspension was vortexed for 5 min after addition of the chloroform-methanol mix. After filtering out the cell debris, 3 mL of deionized water were added to remove the non-lipid constituents of the algal extract via phase separation. The bottom chloroform phase was collected for analysis after the top methanol-water phase was carefully removed.

2.5. ^{31}P NMR analysis of phospholipids

^{31}P NMR analysis was employed to identify and quantify individual algal phospholipids. The analysis was performed in an Inova 400 spectrometer at 25 °C. Deuterated chloroform and analytical grade methanol were obtained from Fisher Scientific (Pittsburg, PA). Analytical standards for the phospholipids phosphatidylcholine (PC), lyso-phosphatidylcholine (lyso-PC), phosphatidylethanolamine (PE), and phosphatidylinositol (PI) were purchased from Sigma (St. Louis, MO).

Each phospholipid standard (100 mg) was dissolved in 3 mL of deuterated chloroform-methanol 2:1 volumetric mixture, as described elsewhere [18]. The samples were placed in 10-mm NMR tubes. The NMR spectra obtained from the analytical standards were utilized to identify the chemical shift δ (ppm) of each phospholipid and to generate calibration curves for determining the cell mass content of PC, lyso-PC, PE, and PI in the VFPPBR microalgal extracts.

2.6. Data analysis

The maximum specific growth rate μ_{max} (d^{-1}) of microalgal growth during VFPPBR cultivations was computed from the slope of the linear regression curves (R^2 = 0.97–0.99, $P < 0.001$) of the natural logarithm of cell concentration (N) versus time (t) using the exponential growth phase data points. The volumetric cell mass productivity P_v ($g{\cdot}L^{-1}{\cdot}d^{-1}$) was calculated from the change in cell mass concentration X ($g{\cdot}L^{-1}$) within a certain cultivation time (d). The areal cell mass productivity P_a ($g{\cdot}m^{-2}{\cdot}d^{-1}$) was computed based on the VFPPBR's measured surface area of 0.094 m^2. The total cell mass yield on nitrogen (Y_N) and phosphorus (Y_P) were computed from the consumed mass of NO_3^--N and consumed mass of PO_4^{3-}-P, respectively. Calculations and statistical analysis were performed using Microsoft Excel's built-in statistical tools.

3. Results and discussion

3.1. Cultivation of N. oculata for phospholipid production

The batch cultivation experiments with *N. oculata* were conducted in the VFPPBR at a working volume of 3.5 L. As described earlier, each run consisted of two phases: (1) Initial cultivation in a macronutrient-rich growth phase to maximize phospholipid production until growth leveled off, at which point 2 L of culture were harvested for subsequent phospholipid extraction and analysis; and (2) Further cultivation of the remaining culture, supplemented with 2 L of fresh medium, but without subsequent nitrate and phosphate supplementation to subject the cells to a starvation period and measure their phospholipid content.

3.1.1. Cultivation at NO_3^-/PO_4^{3-} = 15

N. oculata was cultivated in duplicate in the VFPPBR at a macronutrient mass ratio of 15 (NO_3^-/PO_4^{3-} = 15). This ratio has been employed before to boost volumetric cell mass productivity [25,26]. Culture samples were taken daily and the growth parameters OD_{680}, cell concentration N (cells·mL^{-1}), and dry cell mass X ($g{\cdot}L^{-1}$) were measured. The time progression for each of these parameters is shown in Fig. 2. The growth phase of cultivation in nutrient-rich media lasted 14 days during which the two macronutrients were supplemented at the set ratio to maintain $NO_3^- > 200\,mg{\cdot}L^{-1}$ and $PO_4^{3-} > 10\,mg{\cdot}L^{-1}$. From the exponential portion of the growth phase, the maximum specific growth rate (μ_{max}) of the culture, based on cell concentration (cells·mL^{-1}), was calculated as 0.36 d^{-1}, which is equivalent to a doubling time of 1.9 days, and cell mass concentration reached a maximum of 2.31 $g{\cdot}L^{-1}$. After harvesting 2 L of the culture on the 14th day, the remainder was cultivated for an additional 32 days, but under macronutrient starvation conditions (no further NO_3^- and PO_4^{3-} addition) before the final harvest. As the macronutrients were depleted, cell growth slowed down and ceased completely past the 24th day.

3.1.2. Cultivation at NO_3^-/PO_4^{3-} = 5

N. oculata was cultivated in the VFPPBR in duplicate at a macronutrient mass ratio of 5 (NO_3^-/PO_4^{3-} = 5). This ratio was selected to test our hypothesis that higher presence of phosphorus, which is required for the formation of phospholipids in the cell membrane, will lead to higher phospholipid productivity by the cellular metabolism. Samples were taken daily and the growth parameters OD_{680}, N (cells·mL^{-1}), and X ($g{\cdot}L^{-1}$) were measured to monitor the growth performance of *N. oculata* in the VFPPBR. The time progression for each growth parameter is shown in Fig. 3. The growth phase of cultivation in nutrient-rich media lasted 15 days during which the two macronutrients were supplemented at the set ratio to maintain $NO_3^- > 200\,mg{\cdot}L^{-1}$ and $PO_4^{3-} > 10\,mg{\cdot}L^{-1}$. Interestingly, at NO_3^-/PO_4^{3-} = 5 the maximum specific growth rate (μ_{max}) of the cells was 0.59 d^{-1} (doubling time of 1.2 days), which is 64% faster than at NO_3^-/PO_4^{3-} = 15. The maximum cell mass concentration of 2.11 $g{\cdot}L^{-1}$ at NO_3^-/PO_4^{3-} = 5 was just 9% lower than the 2.31 $g{\cdot}L^{-1}$ achieved at NO_3^-/PO_4^{3-} = 15. The observed specific growth rate values for *N. oculata* are consistent with the previously reported values of 0.16–0.90 d^{-1} [27], 0.15–0.73 d^{-1} [28], and 0.19–0.57 d^{-1} [29]. After

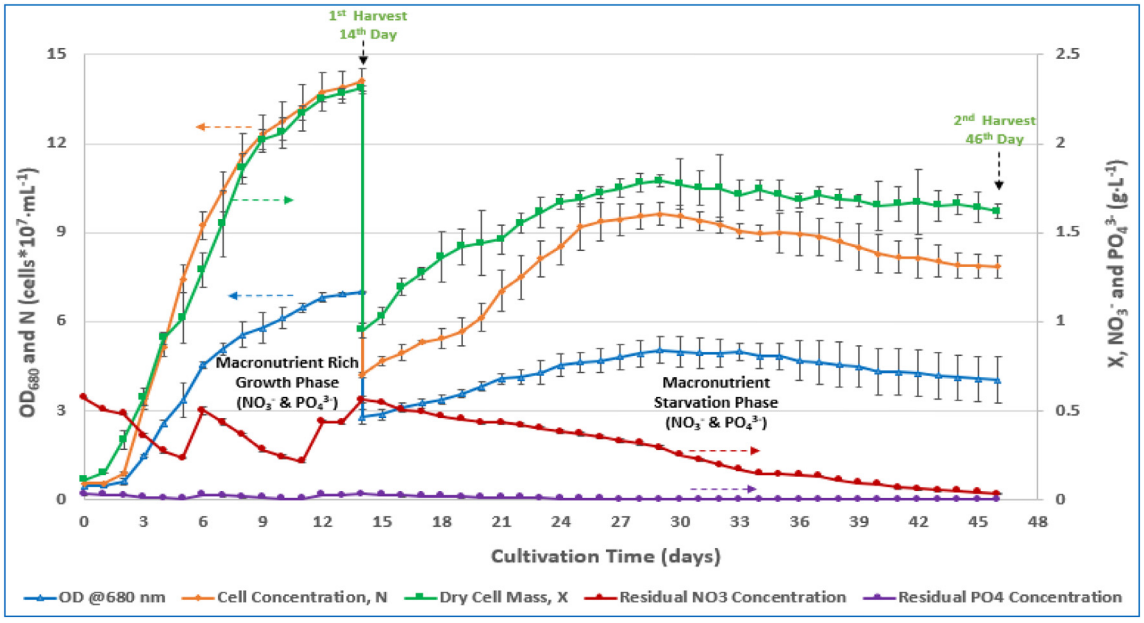

Fig. 2. Cultivation profile at NO_3^-/PO_4^{3-} = 15 during macronutrient-rich growth phase (days 0–14) and macronutrient starvation phase (days 14–46). Error bars represent SD for biological replicates (mean ± SD, n = 2). Mean values of measurement replicates (n = 2) were used with SD not exceeding 13% of the respective mean for any of the monitored culture parameters.

harvesting 2 L of the culture on the 15th day, the remaining 1.5 L was supplemented with 2 L of fresh medium and cultivated for an additional 31 days, but under starvation conditions (no further provision of macronutrients) until the final harvest. After macronutrient depletion, cell growth progressively slowed down until it ceased past the 33rd day.

3.1.3. Comparison of growth performance

Based on the data shown in Figs. 2 and 3, the growth characteristics of *N. oculata* at the macronutrient ratios of 15 and 5 were calculated and summarized in Table 2. As mentioned earlier, at the NO_3^-/PO_4^{3-} ratio of 5, which in essence provided the cells with a 3-fold richer phosphorus environment per unit of nitrogen, the algae grew faster than at the ratio of 15. On the other hand, the maximum dry cell mass concentration (X_{max}), the maximum cell number concentration (N_{max}), and the cell mass productivities (P_V and P_A) were slightly higher at NO_3^-/PO_4^{3-} = 15.

It should be noted that sample analysis for each cultivation indicated the existence of strong linear correlations (not shown) among the three growth parameters OD_{680}, N, and X with statistical values $R^2 > 0.93$, $p < 0.0001$ in all cases. Hence, the least labor-intensive OD_{680} parameter could be used to accurately derive the other two growth parameters (N and X) during lengthy cultivations.

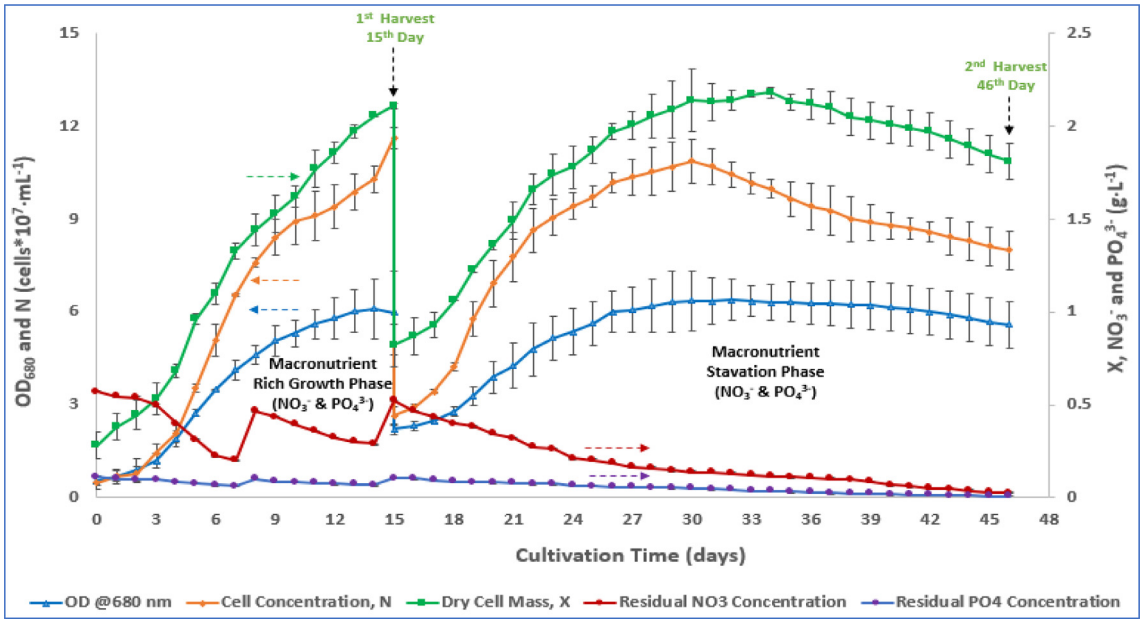

Fig. 3. Cultivation profile at NO_3^-/PO_4^{3-} = 5 during macronutrient-rich growth phase (days 0–15) and macronutrient starvation phase (days 15–46). Error bars represent SD for biological replicates (mean ± SD, n = 2). Mean values of measurement replicates (n = 2) were used with SD not exceeding 18% of the respective mean for any of the monitored culture parameters.

Table 2
Summary of *N. oculata* growth parameters at each of the macronutrient ratios during the macronutrient-rich growth phase. Mean and SD values for biological replicates are shown (mean ± SD, n = 2).

Parameter	NO_3^-/PO_4^{3-} = 15	NO_3^-/PO_4^{3-} = 5	Unit
Cultivation time	46	46	days
X_{max}	2.31 ± 0.01	2.11 ± 0.01	$g{\cdot}L^{-1}$
N_{max}	$(1.41 \pm 0.04) * 10^8$	$(1.13 \pm 0.18) * 10^8$	$cells{\cdot}mL^{-1}$
μ_{max}	0.36 ± 0.04	0.59 ± 0.06	d^{-1}
P_v	157 ± 109	130 ± 61	$mg{\cdot}L^{-1}{\cdot}d^{-1}$
P_a	2.2 ± 1.5	1.8 ± 0.8	$g{\cdot}m^{-2}{\cdot}d^{-1}$
Y_N	7.73 ± 2.20	6.65 ± 0.02	$g{\cdot}g^{-1}$ NO_3^--N
Y_P	73.0 ± 7.4	40.7 ± 1.2	$g{\cdot}g^{-1}$ PO_4^{3-}-P

3.2. Quantification of microalgal phospholipids using ^{31}P NMR spectroscopy

3.2.1. Calibration with phospholipid standards

When phospholipids are analyzed using ^{31}P NMR, each individual phospholipid is identified by its unique chemical shift in the spectrum with high accuracy [18]. ^{31}P NMR spectra of commercial soybean phospholipids analyzed at 25 °C were used as the basis for identifying the individual phospholipids present in the cell mass extract of *N. oculata* harvested from the VFPPBR. The chemical shifts for PC, PE, PI, and lyso-PC were −0.94 ppm, 0.35 ppm, −0.07 ppm, and −0.27 ppm, respectively. In order to quantify each extracted algal phospholipid, calibration plots were created using known concentrations of its commercial counterpart and the area under each peak was correlated to the corresponding concentration. The calibration plots (not shown) demonstrated strong linear correlations.

3.2.2. Effect of macronutrient ratio on phospholipid production

The harvested cultures at the end of the 1st phase (growth) and 2nd phase (starvation) at each of the two NO_3^-/PO_4^{3-} ratios (15 and 5) were centrifuged and processed as described in Section 2.4. The cell extracts in deuterated chloroform-methanol mixture (2:1 volumetrically) were then subjected to ^{31}P NMR analysis to quantify the phospholipid content. The spectra of the analysis are shown in Fig. 4 for each macronutrient ratio (15, 5) and each cultivation phase (growth, starvation).

Using the calibration curves mentioned earlier, the spectral data of Fig. 4 were converted to phospholipid concentrations, as summarized in Table 3. Clearly, the phosphorus-richer environment at NO_3^-/PO_4^{3-} = 5 favors phospholipid production for each of the four phospholipids, when compared to NO_3^-/PO_4^{3-} = 15. This is true both during the nutrient-rich growth phase, when total phospholipid concentration was higher by 26% (22.0 vs. 17.5 $mg{\cdot}L^{-1}$) and during the starvation phase by 44% (19.0 vs. 13.2 $mg{\cdot}L^{-1}$), indicating that phosphorus enrichment during cultivation indeed enhances phospholipid formation. A more extensive study, following the methodology of the present study but with a wider range of macronutrient ratios, can help quantify the dependence of growth rate and phospholipid yield on exogenous phosphate concentration.

The calculated index for each phospholipid as a fraction of total phospholipids is shown in Table 4. During the nutrient-rich growth stage, PC was by far the most prevalent phospholipid at both macronutrient ratios. Starvation, however, led to a significant decrease in PC concentration with consistently a concomitant major increase in PI concentration.

Interestingly, macronutrient starvation appears to have a negative effect on phospholipid production in contrast to a positive effect on total lipids reported in the literature [20–22] and also observed in the present study (Table 4). This negative impact on phospholipids was observed at both macronutrient ratios: at NO_3^-/PO_4^{3-} = 15 the collective phospholipid concentration dropped by 25% after starvation (13.2 vs. 17.5 $mg{\cdot}L^{-1}$) and at NO_3^-/PO_4^{3-} = 5 it dropped by 14% after starvation (19.0 vs. 22.0 $mg{\cdot}L^{-1}$). This suggests that phospholipids

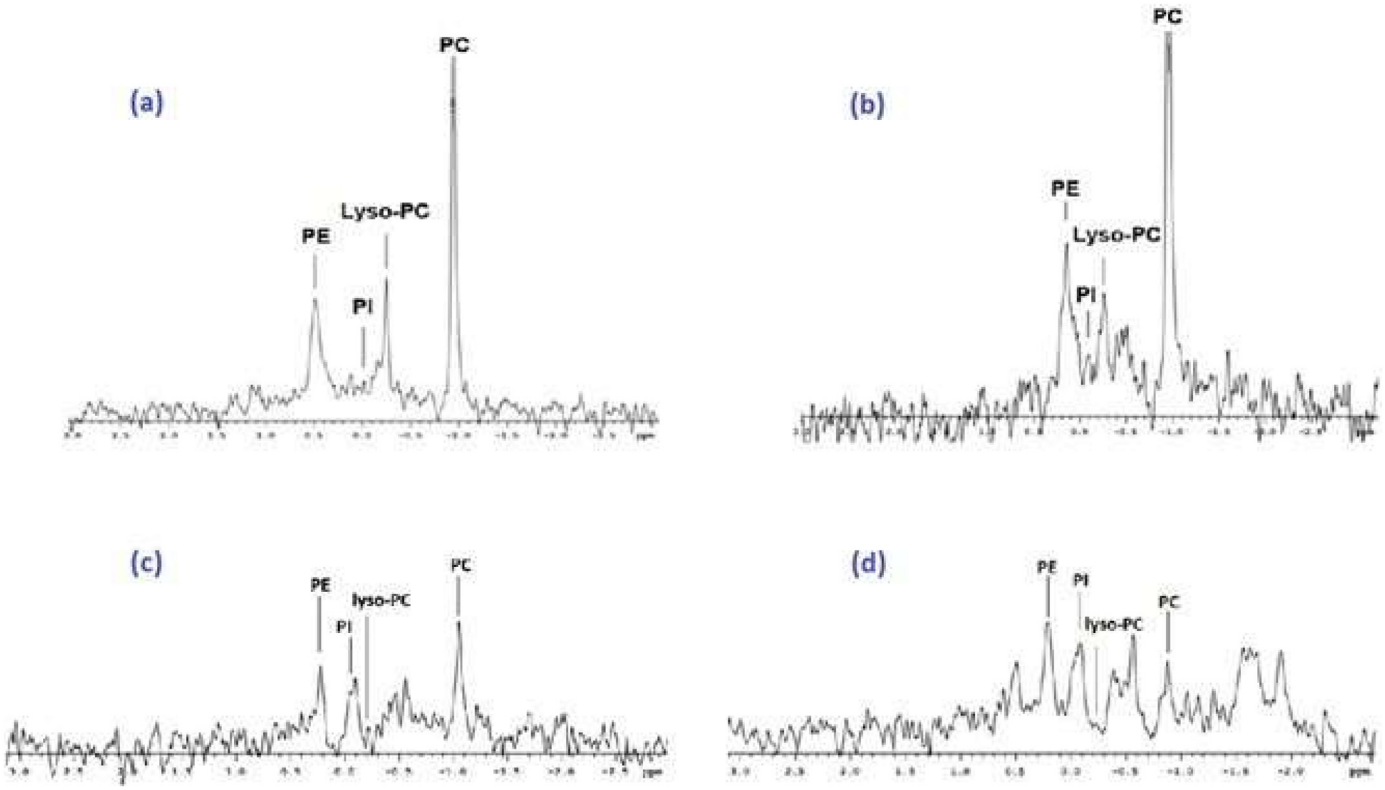

Fig. 4. ^{31}P NMR spectra of *N. oculata* extracts obtained from cell mass at (a) the end of growth phase at NO_3^-/PO_4^{3-} = 15; (b) the end of growth phase at NO_3^-/PO_4^{3-} = 5; (c) the end of starvation phase at NO_3^-/PO_4^{3-} = 15; and (d) the end of starvation phase at NO_3^-/PO_4^{3-} = 5.

Table 3
Quantification of each phospholipid in microalgal extracts via ^{31}P NMR spectroscopy at the respective chemical shift δ (ppm). The concentrations are reported per liter of algal extract dissolved in chloroform. Data replicates are shown as mean ± SD, $n = 2$.

Compound	δ (ppm)	Concentration ($mg \cdot L^{-1}$)			
		Growth phase		Starvation phase	
		$NO_3^-/PO_4^{3-} = 15$	$NO_3^-/PO_4^{3-} = 5$	$NO_3^-/PO_4^{3-} = 15$	$NO_3^-/PO_4^{3-} = 5$
PC	−0.94	14.1 ± 0.8	16.2 ± 0.2	7.7 ± 0.9	7.6 ± 0.4
Lyso-PC	−0.27	1.1 ± 0.2	1.3 ± 0.3	0.2 ± 0.0	0.1 ± 0.0
PE	0.23	0.8 ± 0.5	2.4 ± 0.0	0.9 ± 0.3	1.9 ± 0.1
PI	−0.06	1.5 ± 0.6	2.1 ± 0.1	4.4 ± 0.9	9.4 ± 0.1
Total	–	17.5 ± 2.1	22.0 ± 0.6	13.2 ± 2.1	19.0 ± 0.6

Table 4
Calculated phospholipid indices during the growth and starvation phases at each of the macronutrient ratios based on the data of Table 3 (mean values, n = 2).

Lipid index	$NO_3^-/PO_4^{3-} = 15$		$NO_3^-/PO_4^{3-} = 5$	
	Growth phase	Starvation phase	Growth phase	Starvation phase
PC/TP	0.81	0.59	0.74	0.40
PE/TP	0.04	0.07	0.11	0.10
PI/TP	0.08	0.33	0.10	0.50
Lyso-PC/TP	0.06	0.02	0.06	0.01
TL/biomass	0.31	0.39	0.33	0.41

PC: phosphatidylcholine; PE: phosphatidylethanolamine; PI: phosphatidylinositol; Lyso-PC: lyso-phosphatidylcholine; TP: total phospholipids; TL: total lipids.

should be harvested from the algal cell mass at the end of active growth.

4. Conclusions

Batch cultivation of the microalga *N. oculata* was highly reproducible in a vertical flat panel photobioreactor. The effect of the nitrate-to-phosphate macronutrient ratio on cell growth and phospholipid production was studied at the levels of $NO_3^-/PO_4^{3-} = 15$ and $NO_3^-/PO_4^{3-} = 5$. The specific growth rate of the cells increased at the phosphorus-richer ratio, thus making the cultivation more productive despite a small drop (9%) in the maximum attained dry cell mass concentration.

Using ^{31}P NMR spectroscopy, we measured the concentration of four major algal phospholipids and verified our hypothesis that phosphorus enrichment boosts phospholipid production by the cell metabolism. The productivity of each phospholipid was found to be higher in the phosphorus-richer cultivations (ratio of 5) and collectively 26% higher.

Macronutrient starvation, after a nutrient-rich growth phase, has been reported in the literature as a means of boosting total lipid production in algae at small and large scale. In contrast to total lipids, this technique actually has a negative effect on phospholipid production, possibly because phosphorus is diverted to other cellular functions during phosphate scarcity. Hence, it is recommended that phosphorus enrichment and no subsequent starvation be practiced as a means of maximizing algal phospholipid production.

The data obtained from these batch studies also provide useful guidelines for process development and scale-up of algal phospholipid production. Continuous operation is highly desirable at large scale as a means of achieving higher overall productivity by eliminating the time-consuming start up and shut down periods of batch cultivation. The measured maximum specific growth rate of $0.59\ d^{-1}$ in batch mode can serve as a reference point for selecting an appropriate dilution rate at which to operate future continuous *N. oculata* cultivations in phosphate-rich media.

Acknowledgements

We thank the Patel College of Global Sustainability and the Department of Chemical and Biomedical Engineering at the University of South Florida for their financial support.

Author contribution declaration

All authors, whose names are listed in this manuscript, have made substantial contributions to the conception and design of the study, the acquisition, analysis, and interpretation of data, and the drafting, revising, and final approval of the article. Moreover, all authors take responsibility for the integrity of the work as a whole from inception to finished article and agree to its submission to Algal Research for peer review.

Author interest declaration

All authors, whose names are listed in the manuscript, confirm that there are no known conflicts of interest associated with this publication and there has been no financial support for this work that could have influenced its outcome.

Statement of informed consent and human/animal rights

No conflicts, informed consent, and human or animal rights applicable.

References

[1] M.F. Demirbas, Biofuels from algae for sustainable development, Appl. Energ. 88 (2011) 3473–3480, https://doi.org/10.1016/j.apenergy.2011.01.059.
[2] G. Schroeder, B. Messyasz, B. Łęska, J. Fabrowska, M. Pikosz, A. Rybak, Biomass of freshwater algae as raw material for the industry and agriculture, Przem. Chem. 92 (7) (2013) 1380–1384 https://www.researchgate.net/publication/254258431.
[3] J. Singh, S. Gu, Commercialization potential of microalgae for biofuels production, Renew. Sust. Energ. Rev. 14 (2010) 2596–2610, https://doi.org/10.1016/j.rser.2010.06.014.
[4] W.A. Lecithin, Kirk-Othmer Encyclopedia of Chemical Technology, 5th ed., vol. 20, J. Wiley & Sons, 2004, https://doi.org/10.1002/0471238961.
[5] J. Li, X. Wang, T. Zhang, C. Wang, Z. Huang, X. Luo, Y. Deng, A review on phospholipids and their main applications in drug delivery systems, Asian J. Pharm. Sci. 10 (2) (2015) 81 – 98, https://doi.org/10.1016/j.ajps.2014.09.004.
[6] P. van Hoogevest, B. Prusseit, R. Wajda, Phospholipids: natural functional ingredients and actives for cosmetic products, SOFW-Journal 139 (2013) 8–2013 http://www.lipoid-kosmetik.com/sites/default/files/files/Publikation%20-%20SOFW_8_2013%20Phospholipids(2).pdf.
[7] I.L.D. Olmstead, D.R.A. Hill, D.A. Dias, N.S. Jayasinghe, D.L. Callahan, S.E. Kentish, P.J. Scales, G.J.O. Martin, A quantitative analysis of microalgal lipids for optimization of biodiesel and omega-3 production, Biotechnol. Bioeng. 110 (2013) 2096 – 2104, https://doi.org/10.1002/bit.24844.
[8] A.M.R. Alvarez, M.L.G. Rodríguez, Lipids in pharmaceutical and cosmetic preparations, Grasas Aceites 51 (1–2) (2000) 74–96, https://doi.org/10.3989/gya.2000.v51.i1-2.409.
[9] R.R. dos Santos, D.M. Moreira, C.N. Kunigami, D.A.G. Aranda, C.M.L.L. Teixeira,

Comparison between several methods for total lipid extraction from *Chlorella vulgaris* biomass, Ultrason. Sonochem. 22 (2015) 95 – 99, https://doi.org/10.1016/j.ultsonch.2014.05.015.
[10] E. Ryckebosch, C. Bruneel, R. Termote-Verhalle, K. Muylaert, I. Foubert, Influence of extraction solvent system on extractability of lipid components from different microalgae species, Algal Res. 3 (2014) 36 – 43, https://doi.org/10.1016/j.algal.2013.11.001.
[11] E. Ryckebosch, S.P.C. Bermúdez, R. Termote-Verhalle, C. Bruneel, K. Muylaert, R. Parra-Saldivar, I. Foubert, Influence of extraction solvent system on the extractability of lipid components from the biomass of *Nannochloropsis gaditana*, J. Appl. Phycol. 26 (2014) 1501 – 1510, https://doi.org/10.1007/s10811-013-0189-y.
[12] J. Folch, M. Lees, G.H. Stanley, A simple method for the isolation and purification of total lipids from animal tissues, J. Biol. Chem. 226 (1957) 497 – 509 http://www.jbc.org/content/226/1/497.citation.
[13] E. Ryckebosch, K. Muylaert, M. Eeckhout, T. Ruyssen, I. Foubert, Influence of drying and storage on lipid and carotenoid stability of the microalga *Phaeodactylum tricornutum*, J. Agric. Food Chem. 59 (2011) 11063–11069, https://doi.org/10.1021/jf2025456.
[14] M.A. Borowitzka, N.R. Moheimani, Algae for Biofuels and Energy, 1st ed., Springer, 2013, https://doi.org/10.1007/978-94-007-5479-9.
[15] E. Ryckebosch, K. Muylaert, I. Foubert, Optimization of an analytical procedure for extraction of lipids from microalgae, J. Am. Oil Chem. Soc. 89 (2012) 189 – 198, https://doi.org/10.1007/s11746-011-1903-z.
[16] K. Servaes, M. Maesen, B. Prandi, S. Sforza, K. Elst, Polar lipid profile of *Nannochloropsis oculata* determined using a variety of lipid extraction procedures, J. Agric. Food Chem. 63 (2015) 3931 – 3941, https://doi.org/10.1021/acs.jafc.5b00241.
[17] T.L. Kaduce, K.C. Norton, A.A. Spector, A rapid, isocratic method for phospholipid separation by high-performance liquid chromatography, J. Lipid Res. 24 (1983) 1398–1403 http://www.jlr.org/content/24/10/1398.long.
[18] N. Sotirhos, B. Herslof, L. Kenne, Quantitative analysis of phospholipids by ^{31}P-NMR, J. Lipid Res. 27 (1986) 386–392 http://www.jlr.org/content/27/4/386.full.pdf.
[19] P.R. Cullis, B. De Kruijff, Lipid polymorphism and the functional roles of lipids in biological membranes, Biochim. Biophys. Acta 559 (1979) 399–420, https://doi.org/10.1016/0304-4157(79)90012-1.
[20] I.A. Guschina, J.L. Harwood, Lipids and lipid metabolism in eukaryotic algae, Prog. Lipid Res. 45 (2006) 160–186, https://doi.org/10.1016/j.plipres.2006.01.001.
[21] S.G. Lynn, S.S. Kilham, D.A. Kreeger, S.J. Interlandi, Effect of nutrient availability on the biochemical and elemental stoichiometry in the freshwater diatom *Stephanodiscus minutulus* (Bacillariophyceae), J. Phycol. 36 (2000) 510–522, https://doi.org/10.1046/j.1529-8817.2000.98251.x.
[22] G.A.J. Thompson, Lipids and membrane function in green algae, Biochim. Biophys. Acta 1302 (1996) 17–45, https://doi.org/10.1016/0005-2760(96)00045-8.
[23] S.K. Gupta, A. Malik, F. Bux, Algal Biofuels: Recent Advances and Future Prospects, 1st ed., Springer, 2017, https://doi.org/10.1007/978-3-319-51010-1.
[24] M.L. Kagan, A. Levy, A.A. Leikin-Frenkel, Comparative study of tissue deposition of omega-3 fatty acids from polar-lipid rich oil of the microalgae *Nannochloropsis oculata* with krill oil in rats, Food Funct. 6 (2015) 185–191, https://doi.org/10.1039/C4FO00591K.
[25] A. Ben-Amotz, Effect of irradiance and nutrient deficiency on the chemical composition of *Dunaliella bardawil* Ben-Amotz and Avron (Volvocales, Chlorophyta), J. Plant Phys. 131 (1987) 479 – 487, https://doi.org/10.1016/S0176-1617(87)80290-0.
[26] I. Dogaris, M. Welch, A. Meiser, L. Walmsley, G. Philippidis, A novel horizontal photobioreactor for high-density cultivation of microalgae, Bioresour. Technol. 198 (2015) 316–324, https://doi.org/10.1016/j.biortech.2015.09.030.
[27] R. Chaturvedi, S.R. Uppalapati, M.A. Alamsjah, Y. Fujita, Isolation of quizalofopresistant mutants of *Nannochloropsis oculata* (Eustigmatophyceae) with high eicosapentaenoic acid following *N*-methyl-*N*-nitrosourea-induced random mutagenesis, J. Appl. Phycol. 16 (2004) 135–144, https://doi.org/10.1023/B:JAPH.0000044826.70360.8e.
[28] R. Chaturvedi, Y. Fujita, Isolation of enhanced eicosapentaenoic acid producing mutants of *Nannochloropsis oculata* ST-6 using ethyl methane sulfonate induced mutagenesis techniques and their characterization at mRNA transcript level, Phycol. Res. 54 (2006) 208–219, https://doi.org/10.1111/j.1440-1835.2006.00428.x.
[29] S. Chiu, C. Kao, M. Tsai, S. Ong, C. Chen, C. Lin, Lipid accumulation and CO_2 utilization of *Nannochloropsis oculata* in response to CO_2 aeration, Bioresour. Technol. 100 (2009) 833–838, https://doi.org/10.1016/j.biortech.2008.06.061.